Prostaglandin D_2 as a Mediator of Allergic Asthma

Toshiyuki Matsuoka,[1,2] Masakazu Hirata,[1] Hiroyuki Tanaka,[3] Yoshimasa Takahashi,[3] Takahiko Murata,[1] Kenji Kabashima,[1] Yukihiko Sugimoto,[4] Takuya Kobayashi,[1] Fumitaka Ushikubi,[1] Yoshiya Aze,[5] Naomi Eguchi,[6] Yoshihiro Urade,[6] Nobuaki Yoshida,[7] Kazushi Kimura,[8] Akira Mizoguchi,[8] Yoshihito Honda,[2] Hiroichi Nagai,[3] Shuh Narumiya[1]*

Allergic asthma is caused by the aberrant expansion in the lung of T helper cells that produce type 2 (T_H2) cytokines and is characterized by infiltration of eosinophils and bronchial hyperreactivity. This disease is often triggered by mast cells activated by immunoglobulin E (IgE)–mediated allergic challenge. Activated mast cells release various chemical mediators, including prostaglandin D_2 (PGD_2), whose role in allergic asthma has now been investigated by the generation of mice deficient in the PGD receptor (DP). Sensitization and aerosol challenge of the homozygous mutant ($DP^{-/-}$) mice with ovalbumin (OVA) induced increases in the serum concentration of IgE similar to those in wild-type mice subjected to this model of asthma. However, the concentrations of T_H2 cytokines and the extent of lymphocyte accumulation in the lung of OVA-challenged $DP^{-/-}$ mice were greatly reduced compared with those in wild-type animals. Moreover, $DP^{-/-}$ mice showed only marginal infiltration of eosinophils and failed to develop airway hyperreactivity. Thus, PGD_2 functions as a mast cell–derived mediator to trigger asthmatic responses.

The chronic airway inflammation associated with asthma is characterized by infiltration of both T lymphocytes that produce T_H2 cytokines and eosinophilic leukocytes (*1*). Large numbers of eosinophils and high concentrations of T_H2 cytokines, such as interleukin-4 (IL-4), IL-5, and IL-13, are thus present in both the airway and bronchial alveolar lavage (BAL) fluid of individuals with asthma. The importance of T_H2 cytokines in asthma has been demonstrated in animal models, in which either disruption of the genes encoding these proteins or their antibody-mediated neutralization prevents eosinophilia and attenuates various pathological changes, such as airway hyperreactivity, associated with this condition (*2*). Symptoms of asthma are induced by exposure to specific antigens. Affected individuals produce IgE antibodies to these antigens, and antigen-antibody–mediated cross-linking of the IgE receptors on the surface of mast cells and the consequent activation of these cells are suggested to be important in initiation and development of bronchial asthma (*3*).

Activated mast cells produce a variety of chemical mediators, one of which, prostaglandin D_2 (PGD_2), is the major cyclooxygenase metabolite of arachidonic acid produced by these cells in response to antigen challenge (*4*). PGD_2 is released in large amounts during asthmatic attacks in humans, and it has been proposed as a marker of mast cell activation in asthma (*5*). However, the role of PGD_2 in allergic asthma remains unclear. PGD_2 elicits its biological actions through interaction with the PGD receptor (DP), a heterotrimeric GTP-binding protein–coupled, rhodopsin-type receptor that is specific for this PG (*6*). To clarify the role of PGD_2 in asthma, we generated and characterized mice deficient in DP.

The mouse DP gene was disrupted by insertion of a neomycin resistance gene into the first coding exon (exon 2) (Fig. 1A), and mice chimeric for the resulting mutant allele were generated and mated with C57BL/6 animals to produce mice heterozygous for this allele (*7*). Interbreeding of the heterozygotes produced homozygous mutant ($DP^{-/-}$) mice (Fig. 1B) in a ratio expected from Mendelian inheritance, indicating that the lack of a functional DP gene does not result in fetal death. Reverse transcription and polymerase chain reaction (RT-PCR) analysis confirmed a higher molecular weight transcript corresponding to the Neo-inserted DP mRNA in the homozygous mutants (Fig. 1C). Loss of functional DP protein in these animals was confirmed by a bioassay with tracheal smooth muscle (*8*). Whereas PGD_2 and the DP agonist BW245C [5(6-carboxyhexyl)-1-(3-cyclohexyl-3-hydroxypropyl)hydantoin] (*9*) each induced relaxation of tracheal smooth muscle from wild-type mice, no such effect was apparent in muscle derived from $DP^{-/-}$ animals (Fig. 1D). The $DP^{-/-}$ mice showed no apparent behavioral, anatomic, or histological abnormalities during 1 year of observation under specific pathogen-free conditions. To exclude possible effects

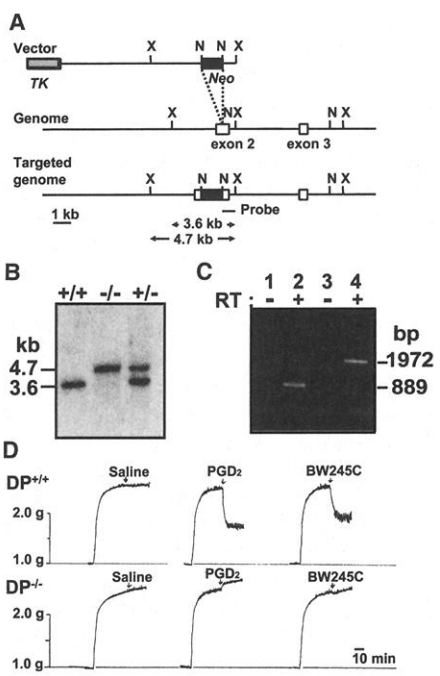

Fig. 1. Disruption of the mouse DP gene. (**A**) Strategy for targeted disruption. Organization of the DP gene, construction of the targeting vector (*TK*, thymidine kinase gene; *Neo*, neomycin resistance gene), and structure of the targeted genome are shown. Restriction sites are indicated: N, Nhe I; and X, Xba I. (**B**) Southern blot analysis. Genomic DNA from newborn littermates of heterozygote intercrosses was digested with Xba I, and the resulting fragments were subjected to analysis with a Nhe I–Xba I fragment of the genomic DNA as a probe. The positions of 3.6-kb (wild-type) and 4.7-kb (mutant) hybridizing fragments are shown for mice of the indicated genotypes. (**C**) RT-PCR analysis. Polyadenylated RNA from the ileum of wild-type mice (lanes 1 and 2) and $DP^{-/-}$ mice (lanes 3 and 4) was subjected to PCR amplification in the absence (lanes 1 and 3) or presence (lanes 2 and 4) of reverse transcriptase (RT). The estimated positions of nucleotides of 1972 and 889 base pairs (bp) are indicated on the right. (**D**) Relaxation of tracheal smooth muscle by PGD_2 or BW245C. Tracheal rings from wild-type (top traces) and $DP^{-/-}$ (bottom traces) mice were suspended in an organ bath and induced to contract with carbachol. Relaxation in response to 3 μM PGD_2 or 100 nM BW245C (or saline) applied at the times indicated by the arrows was assessed.

[1]Department of Pharmacology, [2]Department of Ophthalmology, and [8]Department of Anatomy, Kyoto University Faculty of Medicine, Kyoto 606-8501, Japan. [3]Department of Pharmacology, Gifu Pharmaceutical University, Gifu 502-0003, Japan. [4]Department of Physiological Chemistry, Kyoto University Faculty of Pharmaceutical Sciences, Kyoto 606-8501, Japan. [5]Fukui Safety Research Laboratories, Ono Pharmaceutical Company, Fukui 913-8538, Japan. [6]Osaka Bioscience Institute, Osaka 565-0874, Japan. [7]Institute of Medical Science, University of Tokyo, Tokyo 108-8639, Japan.

*To whom correspondence should be addressed. Department of Pharmacology, Kyoto University Faculty of Medicine, Yoshida, Sakyo-ku, Kyoto 606-8501, Japan. E-mail: snaru@mfour.med.kyoto-u.ac.jp

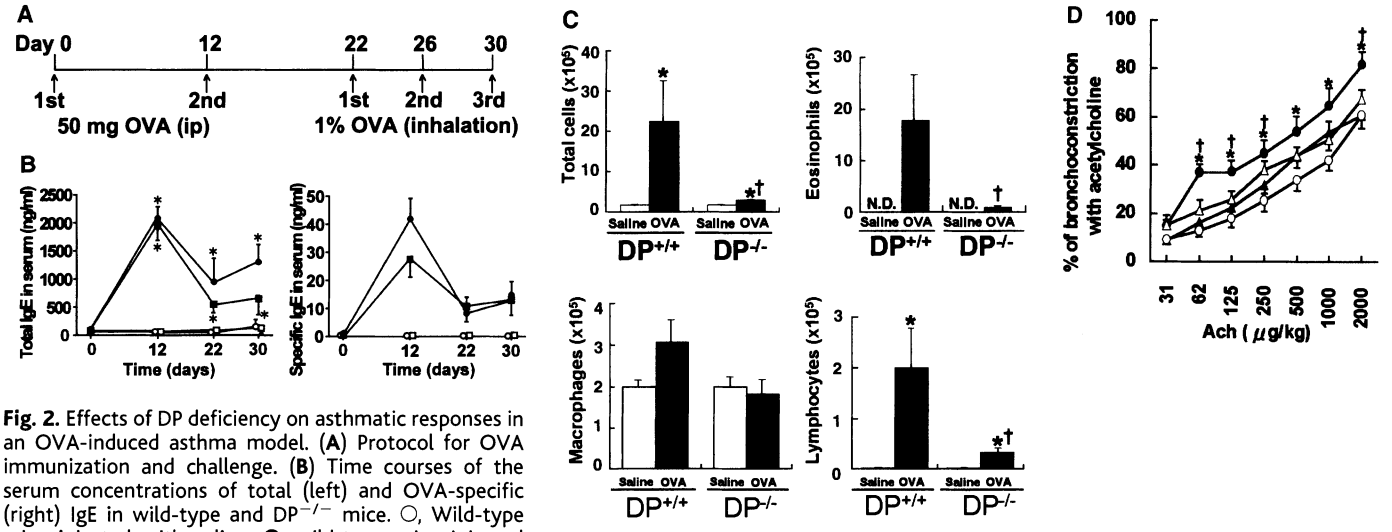

Fig. 2. Effects of DP deficiency on asthmatic responses in an OVA-induced asthma model. (**A**) Protocol for OVA immunization and challenge. (**B**) Time courses of the serum concentrations of total (left) and OVA-specific (right) IgE in wild-type and $DP^{-/-}$ mice. ○, Wild-type mice injected with saline; ●, wild-type mice injected with OVA; □, $DP^{-/-}$ mice injected with saline; ■, $DP^{-/-}$ mice injected with OVA. (**C**) Infiltration of inflammatory cells in BAL fluid. The numbers of total cells (upper left), eosinophils (upper right), macrophages (lower left), and lymphocytes (lower right) recovered in BAL fluid of OVA-challenged or saline-treated wild-type and $DP^{-/-}$ mice are shown. N.D., not detected. (**D**) Reactivity of the airway to acetylcholine in wild-type and DP-deficient mice. The dose-response curves of acetylcholine-induced bronchoconstriction in saline-treated (○) and OVA-challenged (●) wild-type mice and saline-treated (△) and OVA-challenged (▲) $DP^{-/-}$ mice are shown. All data are means ± SEM of values from six mice per group. $*P < 0.05$ versus the respective saline control group; $\dagger P < 0.05$ the OVA-challenged wild-type versus $DP^{-/-}$ mice (*26*).

of genetic background, we backcrossed $DP^{-/-}$ animals with C57BL/6 mice for five generations. The resulting heterozygous mice were intercrossed, and progenies of the resulting wild-type and $DP^{-/-}$ littermates (N_5) were subjected to the analysis below (*10*).

The role of DP in asthma was investigated with an ovalbumin (OVA)-induced asthma model in which PGD_2 is generated in response to antigen challenge, as it is in humans with this condition (*11*). Wild-type and $DP^{-/-}$ mice were sensitized with intraperitoneal (ip) injections of OVA on day 0 and day 12 and were then exposed to aerosolized OVA on days 22, 26, and 30 (Fig. 2A) (*12*); control animals received saline instead of OVA. To determine the efficiency of this sensitization procedure, we analyzed serum concentrations of IgE. The concentrations of both total IgE and OVA-specific IgE in mice were markedly increased in response to ip injection of OVA and were boosted by subsequent inhalation of OVA; no substantial differences were apparent in this regard between wild-type and $DP^{-/-}$ mice (Fig. 2B). Repeated antigen inhalation in immunized wild-type mice resulted in a significant increase in total cell number in BAL fluid compared with that for the corresponding saline-treated control animals [22.2 (±10.4) × 10^5 versus 2.5 (±0.2) × 10^5, $P < 0.05$] (*13*). The infiltrated cells consisted predominantly of eosinophils, although the number of lymphocytes in the BAL fluid was also significantly increased (Fig. 2C). In contrast, only marginal increases in the numbers of eosinophils and lymphocytes in BAL fluid were apparent in $DP^{-/-}$ mice exposed to OVA challenge (Fig. 2C). Repeated OVA challenge in this animal model results in the development of airway hyperreactivity. We measured such hyperreactivity to acetylcholine 24 hours after the third inhalation of antigen (*14*). The OVA challenge significantly increased the sensitivity to acetylcholine in the wild-type mice, whereas little increase was detected in $DP^{-/-}$ animals (Fig. 2D).

Given the essential role of T_H2 cytokines in evoking asthmatic responses (*2*), we measured the concentrations of IL-4, IL-5, and IL-13 in BAL fluid from wild-type and $DP^{-/-}$ mice (*15*). Challenge with OVA induced significant increases in the concentrations of all three of these T_H2 cytokines in BAL fluid from wild-type mice (Fig. 3, A through C). Antigen challenge also increased the concentrations of these cytokines in $DP^{-/-}$ mice, but to a significantly lesser extent than in wild-type mice. In contrast, OVA challenge induced no difference in the concentration of the T_H1 cytokine interferon-γ (IFN-γ) in BAL fluid between wild-type and homozygous DP-deficient mice (Fig. 3D).

In humans with asthma, infiltration of numerous lymphocytes is apparent in the lung and is thought to be responsible for the increased abundance of T_H2 cytokines. Lymphocytes and eosinophils accumulate in the bronchial submucosa and around blood vessels and, in some areas, lymphocytes form bronchus-associated lymphoid tissue (BALT). Histological analysis of OVA-challenged wild-type mice revealed

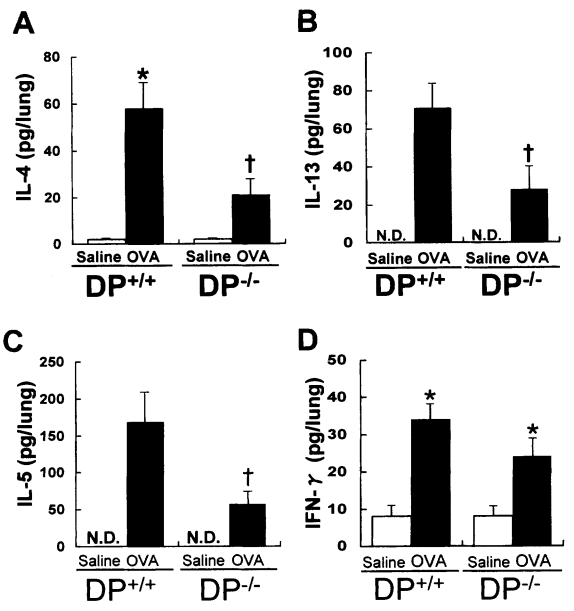

Fig. 3. Effects of OVA challenge on cytokine concentrations in BAL fluid of wild-type and $DP^{-/-}$ mice. The amounts of IL-4 (**A**), IL-13 (**B**), IL-5 (**C**), and IFN-γ (**D**) are expressed as means ± SEM of values from 10 mice per group. N.D., not detected. $*P <$ 0.05 versus the respective saline control group; $\dagger P < 0.05$ versus the OVA-challenged wild-type mice (*26*).

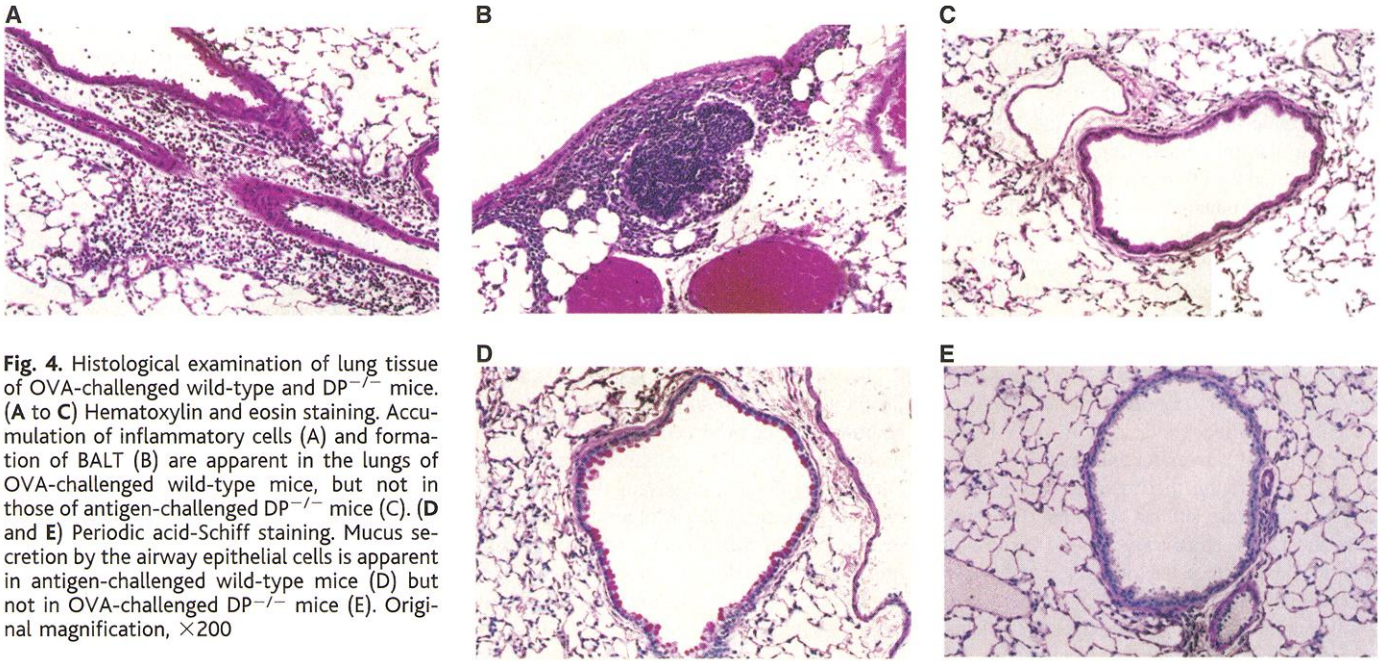

Fig. 4. Histological examination of lung tissue of OVA-challenged wild-type and $DP^{-/-}$ mice. (**A** to **C**) Hematoxylin and eosin staining. Accumulation of inflammatory cells (A) and formation of BALT (B) are apparent in the lungs of OVA-challenged wild-type mice, but not in those of antigen-challenged $DP^{-/-}$ mice (C). (**D** and **E**) Periodic acid-Schiff staining. Mucus secretion by the airway epithelial cells is apparent in antigen-challenged wild-type mice (D) but not in OVA-challenged $DP^{-/-}$ mice (E). Original magnification, ×200

extensive cell infiltration (Fig. 4A) and occasional BALT formation (Fig. 4B) in the lungs of all animals (*16*). In contrast, little cell infiltration was detected in the lungs of OVA-challenged $DP^{-/-}$ animals (Fig. 4C). We next examined mucus secretion by airway epithelial cells, given that hypersecretion of mucus is one of the characteristic features of asthmatic airways both in humans and animal models (*17*). Whereas many mucus-containing cells were apparent in wild-type mice challenged with OVA (Fig. 4D), few such cells were detected in antigen-challenged $DP^{-/-}$ mice (Fig. 4E).

Finally, we examined the expression and localization of DP in the lung. Northern blot analysis (*7*) detected little expression of DP in the lung of nonimmunized as well as immunized mice before the antigen challenge (Fig. 5A). However, the OVA challenge to the airway markedly enhanced the DP expression in the lung. No induction was found in the spleen before and after the antigen challenge. We next performed immunofluorescence and immunoelectron microscopy using a specific antibody to mouse DP (*18*). Weak DP receptor immunoreactivity was detected in the cells surrounding bronchioles and alveoli of the lung of the immunized wild-type mouse before challenge, and the immunoreactivity was markedly enhanced by the airway exposure to OVA (Fig. 5B). In contrast, no DP receptor immunoreactivity was detected in the lung of $DP^{-/-}$ mice

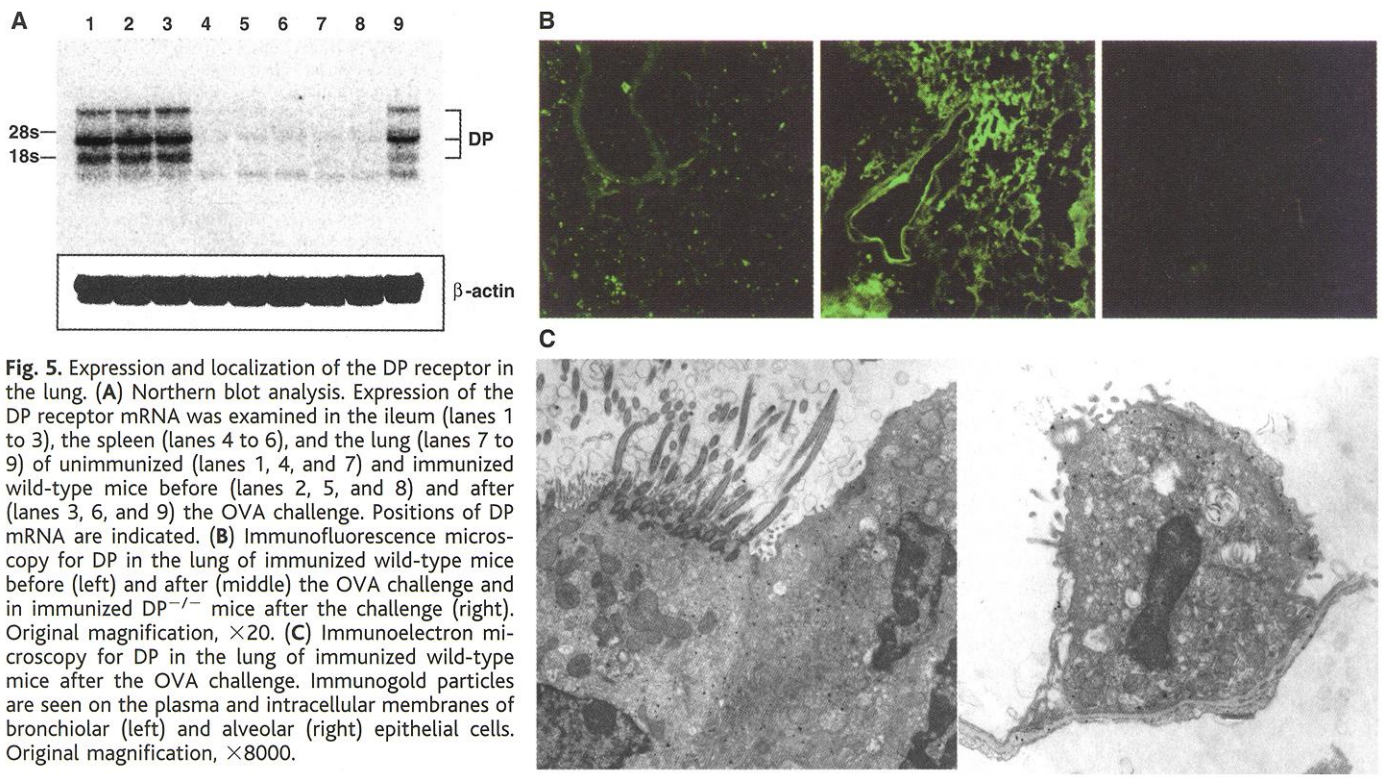

Fig. 5. Expression and localization of the DP receptor in the lung. (**A**) Northern blot analysis. Expression of the DP receptor mRNA was examined in the ileum (lanes 1 to 3), the spleen (lanes 4 to 6), and the lung (lanes 7 to 9) of unimmunized (lanes 1, 4, and 7) and immunized wild-type mice before (lanes 2, 5, and 8) and after (lanes 3, 6, and 9) the OVA challenge. Positions of DP mRNA are indicated. (**B**) Immunofluorescence microscopy for DP in the lung of immunized wild-type mice before (left) and after (middle) the OVA challenge and in immunized $DP^{-/-}$ mice after the challenge (right). Original magnification, ×20. (**C**) Immunoelectron microscopy for DP in the lung of immunized wild-type mice after the OVA challenge. Immunogold particles are seen on the plasma and intracellular membranes of bronchiolar (left) and alveolar (right) epithelial cells. Original magnification, ×8000.

before and after the challenge. These results not only verified that our gene-targeting strategy successfully disrupted the DP gene, but also confirmed the induction of the DP receptor in the asthmatic lung suggested by the Northern blot analysis. Immunoelectron microscopy further identified the DP receptor–expressing cells as ciliated and nonciliated epithelial cells in the bronchioles and type II alveolar epithelial cells (Fig. 5C). Moderate DP receptor immunoreactivity was also detected in the type I alveolar epthelial cells and infammatory white blood cells (*19*).

We have shown that $DP^{-/-}$ mice do not develop asthmatic responses in an OVA-induced asthma model, indicating that PGD_2 and its receptor (DP) are important for such responses. Our observation that the serum concentrations of IgE were similar in immunized wild-type and $DP^{-/-}$ mice suggests that the loss of DP does not affect the primary immune response. Indeed, OVA induced the production of similar amounts of T_H2 cytokines by splenocytes prepared from immunized wild-type and $DP^{-/-}$ mice (*19*). In contrast, the concentrations of such cytokines in BAL fluid after OVA challenge were significantly lower in $DP^{-/-}$ mice than in wild-type mice, suggesting that the effect of DP deficiency is manifested locally at the site of challenge. The absence of lymphocyte accumulation in OVA-challenged $DP^{-/-}$ mice is suggestive of a defect in the recruitment of lymphocytes to the site of allergen challenge. Eosinophilic infiltration in allergic asthma is thought to be a consequence of the activation of T_H2 lymphocytes. Consistent with this notion, infiltration of eosinophils did not occur to a significant extent in OVA-challenged $DP^{-/-}$ mice. Furthermore, the in vivo administration of PGD_2 into the airway of dogs induced marked eosinophilic infiltration (*20*). Transgenic expression of PGD synthetase in the lung also increased both the concentrations of IL-4 and IL-5 and the extent of eosinophilic infiltration in BAL fluid in a mouse OVA-induced asthma model (*21*). These various observations suggest that PGD_2 produced in response to allergic challenge acts at DP in the lung to recruit lymphocytes to the site of challenge. Indeed, we observed the marked expression of the DP receptor in bronchiolar and alveolar epithelial cells in the asthmatic airway. The airway epithelium is proposed as a source of proinflammatory cytokines and chemokines in asthma (*3*), raising the possibility that PGD_2 acting at DP in the epithelium may stimulate the production and release of these mediators.

Is PGD_2 the sole, obligatory mediator of asthma? Although individuals with asthma usually exhibit high concentrations of IgE in serum, the IgE concentration is often not correlated with the incidence of asthma attacks. This dissociation has led to the suggestion that the IgE- and mast cell–mediated pathway is important in triggering asthma, but plays a limited role in the chronic phase of an established asthmatic state. The mast cell–derived PGD_2 therefore appears to play an important role that is restricted to the initiation process, and other redundant pathways that evoke asthmatic responses exist. Consistently, we have found that excessive challenge with OVA overcomes the effect of DP deficiency (*22*). It is also possible that PGD_2 produced by cells other than mast cells during asthmatic attacks contributes to trigger and/or enhance allergic responses. It was reported that PGD_2 is produced also by macrophages and dendritic cells (*23*).

In summary, we have shown that PGD_2 functions as a mediator of allergic asthma. In addition to being produced in the lung, PGD_2 is produced in various other tissues in response to allergic stimuli (*24*), suggesting that it may also play an important role in other allergic disorders, such as allergic rhinitis and atopic dermatitis. The DP receptor may thus represent a new therapeutic target for the treatment of such allergic reactions (*25*).

References and Notes

1. J. Bousquet *et al.*, *N. Engl. J. Med.* **323**, 1033 (1990); D. S. Robinson *et al.*, *N. Engl. J. Med.* **326**, 298 (1992).
2. P. S. Foster, S. P. Hogan, A. J. Ramsay, K. I. Matthaei, I. G. Young, *J. Exp. Med.* **183**, 195 (1996); D. B. Corry *et al.*, *Mol. Med.* **4**, 344 (1998); M. Wills-Karp *et al.*, *Science* **282**, 2258 (1998); G. Grünig *et al.*, *Science* **282**, 2261.
3. S. T. Holgate, *Clin. Exp. Allergy* **28** (suppl. 5), 97 (1998).
4. R. A. Lewis and K. F. Austen, *Nature* **293**, 103 (1981); L. J. Roberts II, B. J. Sweetman, R. A. Lewis, K. F. Austen, J. A. Oates. *N. Engl. J. Med.* **303**, 1400 (1980).
5. J. J. Murray *et al.*, *N. Engl. J. Med.* **315**, 800 (1986); M. C. Liu *et al.*, *Am. Rev. Respir. Dis.* **142**, 126 (1990); S. E. Wenzel, J. Y. Westcottt, G. L. Larsen, *J. Allergy Clin. Immunol.* **87**, 540 (1991); S. O'Sullivan, *Acta Physiol. Scand. Suppl.* **644**, 1 (1999).
6. M. Hirata, A. Kakizuka, M. Aizawa, F. Ushikubi, S. Narumiya, *Proc. Natl. Acad. Sci. U.S.A.* **91**, 11192 (1994).
7. Murine DP genomic clones were isolated from a 129/Sv genomic DNA library (Stratagene) with the corresponding cDNA as a probe. The targeting vector was constructed by inserting the neomycin resistance gene (pMC1-neo, Stratagene) into a unique Nhe I site of the first coding exon; this insertion disrupts the DP gene in the sequence encoding the third transmembrane domain of the protein. The herpes simplex virus thymidine kinase gene was inserted upstream. The targeting vector was linearized and introduced into E14-1 embryonic stem cells from 129/Ola mice by electroporation. Clones resistant to both G418 and gancyclovir were isolated and screened for homologous recombination by PCR amplification. Recombination was then confirmed by Southern blot hybridization. Two lines of embryonic stem cells were injected into C57BL/6 blastocysts to generate chimeric male offspring, which were then mated with C57BL/6 females. Pups with an agouti coat were genotyped by Southern blot analysis for determination of germ line transmission. Polyadenylated RNA was prepared from various organs, which were rapidly removed and homogenized in 10 volumes of Trizol (Gibco-BRL) with a Polytron homogenizer. RT-PCR analysis was performed with 10 μg of polyadenylated RNA with the forward primer, 5′-TCGGTCTTTTATGTGCTCGTG-3′, corresponding to amino acids 57 to 63 in the first coding exon, and the reverse primer, 5′-TCCACGTTACTTTGCTGGGAA-3′, corresponding to amino acids 346 to 353 in the second coding exon. Northern blot analysis was performed on 10 μg of polyadenylated RNA as described [H. Oida *et al.*, *FEBS Lett.* **417**, 53 (1997)].
8. A tracheal ring 4 mm in length was prepared and mounted on a pair of wires under a load of 1.0 g in an organ bath filled with Krebs-Henseleit buffer equilibrated with 95% O_2 and 5% CO_2 at 37°C. Contraction of the ring was induced with 0.2 μM carbachol, and relaxation in response to PGD_2 or BW245C was measured.
9. H. Giles, P. Leff, M. L. Bolofo, M. G. Kelly, A. D. Robertson, *Br. J. Pharmacol.* **96**, 291 (1989).
10. In a separate series of experiments, the progeny of F_2 littermates with a 129/Sv × C57BL/6 mixed background was analyzed, with results almost identical to those obtained with the N_5 littermates.
11. A. F. Walls *et al.*, *Lung* **169**, 227 (1991); N. C. Turner and C. T. Dollery, *Br. J. Pharmacol.* **93**, 751 (1988).
12. H. Tanaka, H. Nagai, Y. Maeda, *Life Sci.* **62**, 169 (1998).
13. Mice were killed by ip injection of sodium pentobarbital (100 mg per kilogram of body mass) 24 hours after the last OVA inhalation. The trachea was cannulated, and the lung was lavaged four times with 1 ml of Ca^{2+}- and Mg^{2+}-free phosphate-buffered saline (PBS) containing 0.1% (w/v) bovine serum albumin and 0.05 mM EDTA. The BAL fluid obtained from each animal was pooled and centrifuged at 150*g* for 10 min at 4°C. Cell pellets were resuspended in the same solution, and the number of nucleated cells staining with Türk solution was counted. Smears of cell suspensions were prepared with the use of a Cytospin II cytocentrifuge, stained with May-Grü-wald-Giemsa dye, and subjected to a differential count of at least 300 cells under a microscope.
14. Mice were anesthetized with sodium pentobarbital (80 mg/kg, ip), and the tail vein was cannulated. The animals were injected intravenously with pancuronium bromide (0.1 mg/kg) and ventilated with the aid of a rodent ventilator at a rate of 60 strokes per minute and a stroke volume of 0.6 ml of air supplemented with oxygen. Airway resistance was measured according to the overflow method described by H. Konzett and R. Rössler [*Arch. Exp. Pathol. Pharmakol.* **195**, 71 (1940)] with the use of a Ugo Basil 7020 bronchospasm transducer connected to the tracheal cannula. Increasing doses of acetylcholine (31.25 to 2000 μg/kg) were injected into the tail vein, and the changes in overflow volume were determined. The increase in respiratory overflow volume induced by acetylcholine was expressed as a percentage of the maximal overflow volume obtained by clamping the tracheal cannula.
15. BAL fluid was collected from wild-type and $DP^{-/-}$ mice 8 hours after the last inhalation of OVA, and the concentrations of IL-4, IL-5, IL-13, and IFN-γ in the fluid were determined by enzyme-linked immunosorbent assay.
16. Twenty-four hours after the last OVA inhalation, mice were anesthetized with sodium pentobarbital, and 10% (v/v) formalin in PBS was infused into the lung for fixation. The lung was then sectioned and stained either with hematoxylin and eosin or with periodic acid-Schiff reagent.
17. T. Aikawa *et al.*, *Chest* **101**, 916 (1992); J. A. Rankin *et al.*, *Proc. Natl. Acad. Sci. U.S.A.* **93**, 7821 (1996).
18. A. Mizoguchi *et al.*, *Proc. Natl. Acad. Sci. U.S.A*, in press.
19. T. Matsuoka *et al.*, unpublished data.
20. D. L. Emery, T. D. Djokic, P. D. Graf, J. A. Nadel, *J. Appl. Physiol.* **67**, 959 (1989).
21. Y. Fujitani and Y. Urade, unpublished data.
22. The effect of DP deficiency was dependent on the strength of antigen challenge. For standard OVA challenges that induced cell infiltration in the BAL fluid of wild-type mice of less than 20×10^5 cells (*2*), a pronounced inhibition of infiltration was apparent in $DP^{-/-}$ mice. However, for excessive OVA challenges that induced infiltration of $\sim 70 \times 10^5$ cells in wild-type mice, a similar number of cells was detected in the BAL fluid of $DP^{-/-}$ mice.
23. Y. Urade, M. Ujihara, Y. Horiguchi, K. Ikai, O. Hayaishi, *J. Immunol.* **143**, 2982 (1989).
24. K. Ikai, K. Danno, T. Horio, S. Narumiya, *J. Invest. Dermatol.* **85**, 82 (1985); R. M. Barr *et al.*, *Br. J. Pharmacol.* **94**, 773 (1988); P. H. Howarth, *Allergy* **52**, 12 (1997).

25. T. Tsuri *et al.*, *J. Med. Chem.* **40**, 3504 (1997).
26. Statistical significance was evaluated by one-way analysis of variance followed by Student's *t* test for unpaired values.

27. We thank K. Ishikawa, Y. Kataoka, K. Deguchi, and T. Obata for technical assistance; T. Arai and H. Nose for secretarial assistance; T. Tanaka and M. Kitaichi for discussions; and O. Hayaishi for encouragement. Supported in part by grants from the Uehara Memorial Foundation and the Smoking Research Foundation.

17 November 1999; accepted 3 February 2000

Facile Detection of Mitochondrial DNA Mutations in Tumors and Bodily Fluids

Makiko S. Fliss,[1] Henning Usadel,[1] Otávia L. Caballero,[1] Li Wu,[1] Martin R. Buta,[1] Scott M. Eleff,[2] Jin Jen,[1] David Sidransky[1]*

Examination of human bladder, head and neck, and lung primary tumors revealed a high frequency of mitochondrial DNA (mtDNA) mutations. The majority of these somatic mutations were homoplasmic in nature, indicating that the mutant mtDNA became dominant in tumor cells. The mutated mtDNA was readily detectable in paired bodily fluids from each type of cancer and was 19 to 220 times as abundant as mutated nuclear p53 DNA. By virtue of their clonal nature and high copy number, mitochondrial mutations may provide a powerful molecular marker for noninvasive detection of cancer.

The human mitochondrial (mt) genome is small (16.5 kb) and encodes 13 respiratory chain subunits, 22 transfer RNAs (tRNAs), and two ribosomal RNAs (rRNAs). Mitochondrial DNA is present at extremely high levels (10^3 to 10^4 copies per cell), and the vast majority of these copies are identical (homoplasmic) at birth (*1*). Expression of the entire complement of mt genes is required to maintain proper function of the organelle, suggesting that even slight alterations in DNA sequences could have profound effects (*2*). It is generally accepted that mtDNA mutations are generated during oxidative phosphorylation through pathways involving reactive oxygen species (ROS). These mutations may accumulate in part because mitochondria lack protective histones and the highly efficient DNA repair mechanisms that are seen in the nucleus (*3*).

Recently, several mtDNA mutations were found specifically in human colorectal cancer (*4*). To determine whether mt mutations could be identified in other cancer types, we studied primary bladder (n = 14), head and neck (n = 13), and lung (n = 14) tumors (*5*). Eighty percent of the mt genome of all the primary tumor samples was polymerase chain reaction (PCR) amplified (*6*) and sequenced manually (Fig. 1). Tumor mtDNA was compared with mtDNA from paired blood samples in all cases and mtDNA from corresponding normal tissue when available (*7*). Of the 292 sequence variants detected, 196 were previously recorded polymorphisms (*2, 8*), whereas 57 were previously unknown polymorphisms (Web table 1) (*9*). The remaining 39 variants were acquired (somatic) mutations identified in 64% (9 of 14) of the bladder cancer patients, 46% (6 of 13) of the head and neck cancer patients, and 43% (6 of 14) of the lung cancer patients (Table 1). Most of these mutations were T-to-C and G-to-A base transitions, indicating possible exposure to ROS-derived mutagens (*10*). Similar to the previous observation by Polyak *et al.* (*4*), the majority of the somatic mutations identified here were also homoplasmic in nature. In addition, several of the bladder and head and neck cancers studied here (Table 1) had multiple mutations, implying possible accumulation of mtDNA damage.

In the bladder tumors, mutation hot spots were primarily in the NADH (reduced form of nicotinamide adenine dinucleotide) dehydrogenase subunit 4 (*ND4*) gene (35%) and in the displacement-loop (D-loop) region (30%). The D-loop region is a critical site for both replication and expression of the mt genome because it contains the leading-strand origin of replication and the major promoters for transcription (*11*). Many (73%) of the mutations identified within protein-coding regions were silent, except for a (Val → Ala) substitution in the NADH dehydrogenase subunit 3 *(ND3)* and a seven–amino acid deletion in cytochrome b (*Cyt b*). The D-loop region was also commonly mutated in the head and neck cancer patients (67%). Two of the head and neck tumors (22%) contained mutations in the *ND4* gene at nucleotide pairs (nps) 10,822 and 11,150, resulting in amino acid substitution of Thr → Met and Ala → Thr, respectively. A similar tendency was observed in the lung cancer patients, demonstrating a high concentration of mutations in the D-loop region (70%).

We hypothesized that the homoplasmic nature of these mutations would make them readily detectable in paired bodily fluids. To test this, we extracted and directly amplified mtDNA from urine samples from patients diagnosed with bladder cancer. All three corresponding urine samples available in this study contained the mutant mtDNA derived from tumor tissues. For example, the mtDNA from a urine sample from bladder cancer patient 799 showed the same nucleotide transition (G → A) as seen in the tumor (Fig. 2A). In all cases, the urine sample contained a relatively pure population of tumor-derived mtDNA, comparable to that of the microdissected tumor sample. Consistent with this observation, saliva samples obtained from head and neck cancer patients contained no detectable wild-type signals (Fig. 2, B and C). By sequence analysis alone, we were able to detect mtDNA mutations in 67% (6 of 9) of saliva samples from head and neck cancer patients. In lung cancer cases, we were initially unable to identify mutant bands from paired bronchoalveolar lavage (BAL) fluids because of the substantial dilution of neoplastic cells in BAL fluid (*12*) (Fig. 2D). Thus, we applied a more sensitive oligonucleotide-mismatch ligation assay to detect mutated mtDNA. As shown in Fig. 3, both lung cancer mutations (arrows) were confirmed in tumor mtDNA with more dilute signals in the corresponding BAL samples and no signal in the corresponding normal

[1]Department of Otolaryngology–Head and Neck Surgery, Head and Neck Cancer Research Division, [2]Department of Anesthesiology and Critical Care Medicine, Johns Hopkins University School of Medicine, Baltimore, MD 21205, USA.

*To whom correspondence should be addressed. E-mail: dsidrans@jhmi.edu

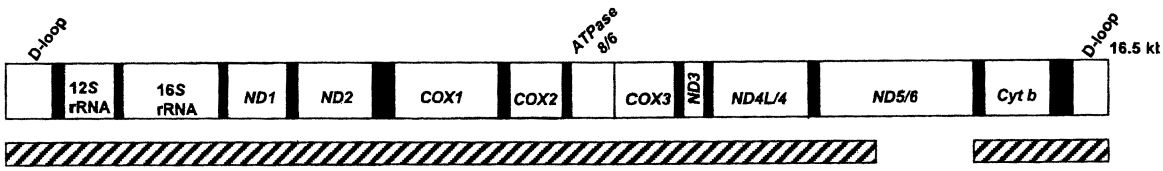

Fig. 1. Schematic representation of a linearized mt genome. Hatched bars indicate the regions sequenced in this study, and solid bars indicate the positions of tRNAs. rRNA, ribosomal RNA; *ND*, NADH dehydrogenase; *COX*, cytochrome c oxidase; *Cyt b*, cytochrome b; *ATPase*, ATP synthase.